

# Planar CuO<sub>2</sub> hole density estimation in multilayered high- $T_c$ cuprates

Sunao Shimizu,\* Shiho Iwai, Shin-ichiro Tabata, Hidekazu Mukuda, and Yoshio Kitaoka  
*Department of Materials Engineering Science, Osaka University, Osaka 560-8531, Japan*

Parasharam M. Shirage, Hijiri Kito, and Akira Iyo

*National Institute of Advanced Industrial Science and Technology (AIST), Umezono, Tsukuba 305-8568, Japan*

(Dated: June 5, 2018)

We report that planar CuO<sub>2</sub> hole densities in high- $T_c$  cuprates are consistently determined by the Cu-NMR Knight shift. In single- and bi-layered cuprates, it is demonstrated that the spin part of the Knight shift  $K_s(300\text{ K})$  at room temperature monotonically increases with the hole density  $p$  from underdoped to overdoped regions, suggesting that the relationship of  $K_s(300\text{ K})$  vs.  $p$  is a reliable measure to determine  $p$ . The validity of this  $K_s(300\text{ K})$ - $p$  relationship is confirmed by the investigation of the  $p$ -dependencies of hyperfine magnetic fields and of spin susceptibility for single- and bi-layered cuprates with tetragonal symmetry. Moreover, the analyses are compared with the NMR data on three-layered Ba<sub>2</sub>Ca<sub>2</sub>Cu<sub>3</sub>O<sub>6</sub>(F,O)<sub>2</sub>, HgBa<sub>2</sub>Ca<sub>2</sub>Cu<sub>3</sub>O<sub>8+ $\delta$</sub> , and five-layered HgBa<sub>2</sub>Ca<sub>4</sub>Cu<sub>5</sub>O<sub>12+ $\delta$</sub> , which suggests the general applicability of the  $K_s(300\text{ K})$ - $p$  relationship to multilayered compounds with more than three CuO<sub>2</sub> planes. We remark that the measurement of  $K_s(300\text{ K})$  enables us to separately estimate  $p$  for each CuO<sub>2</sub> plane in multilayered compounds, where doped hole carriers are inequivalent between outer CuO<sub>2</sub> planes and inner CuO<sub>2</sub> planes.

## INTRODUCTION

In hole doped high- $T_c$  cuprates, the hole density  $p$  in CuO<sub>2</sub> planes has been determined by various methods: indirect chemical methods like solid solutions [1–4], bond valence sums determined from structural bond lengths [5–7], or the Fermi surface topology [8]. Moreover, the thermoelectric power is a universal function of  $p$  [9, 10], and the phase diagram for hole doped cuprates is well described by  $T_c=T_{c,max}[1 - 82.6(p - 0.16)^2]$  [11], which is applicable for the estimation of  $p$  when suitable structural data are not available. These methods are, however, inapplicable when we deal with multilayered compounds because they are composed of more than two inequivalent CuO<sub>2</sub> planes in a unit cell (see Fig. 3(a) as an example). In multilayered cuprates, doped hole carriers are inequivalent between outer CuO<sub>2</sub> planes (OPs) and inner CuO<sub>2</sub> planes (IPs) due to the imbalance of the Madelung potential on each CuO<sub>2</sub> plane; the above-mentioned methods would evaluate not *each hole density* inherent to CuO<sub>2</sub> planes but a *total hole density*. Precise determination of hole density on respective CuO<sub>2</sub> planes is indispensable for gaining deep insight into the phenomena observed in multilayered cuprates [12–16].

It is known that the spin part of the Knight shift  $K_s(300\text{ K})$  at room temperature increases with  $p$  in hole doped cuprates [13, 17–22]. The  $K_s(300\text{ K})$  for OP and IP are separately determined by Cu-NMR. Therefore, each value of  $p$  for OP and for IP can be estimated if the relationship between  $K_s(300\text{ K})$  and  $p$  is established. Meanwhile, a linear equation  $p=0.502K_s(300\text{ K})+0.0462$  has been reported [13, 23], where  $p$  was derived from the NQR frequencies of Cu and O in CuO<sub>2</sub> planes [24]. The values of  $p$  estimated by the linear equation, however, seem relatively large. For example,

an optimal doping level has been evaluated to be  $p \sim 0.22$ - $0.24$  in five-layered Hg-based compounds [14], the value of which is larger than a widely-accepted optimal doping level in hole-doped cuprates,  $p \sim 0.16$ . This inconsistency is probably, in part, due to the calculation that connects NQR frequencies to  $p$  [25]. In addition to that, it is nontrivial whether the  $p$ -dependence of  $K_s(300\text{ K})$  is described with a single equation which holds among different materials.  $K_s$  is proportional to spin susceptibility  $\chi_s$  and hyperfine coupling constants  $A_{hf}$  as  $K_s=A_{hf}\chi_s$ , where the supertransferred magnetic field  $B$  in  $A_{hf}=A+4B$  depends on the materials [26].

In this paper, we report that the planar CuO<sub>2</sub> hole density  $p$  in high- $T_c$  cuprates is consistently evaluated from the spin part of the <sup>63</sup>Cu-Knight shift  $K_s(300\text{ K})$  at room temperature. We show the  $p$  dependences of  $K_s(300\text{ K})$  and of  $B$  in bi-layered Ba<sub>2</sub>CaCu<sub>2</sub>O<sub>4</sub>(F,O)<sub>2</sub> (0212F), together with other single- and bi-layered materials with tetragonal symmetry. NMR data on three-layered Ba<sub>2</sub>Ca<sub>2</sub>Cu<sub>3</sub>O<sub>6</sub>(F,O)<sub>2</sub> (0223F), HgBa<sub>2</sub>Ca<sub>2</sub>Cu<sub>3</sub>O<sub>8+ $\delta$</sub>  (Hg1223) [27], and HgBa<sub>2</sub>Ca<sub>4</sub>Cu<sub>5</sub>O<sub>12+ $\delta$</sub>  (Hg1245) [28] suggest that the  $p$ -dependencies of  $K_s(300\text{ K})$  and of  $B$  hold in multilayered compounds as well. These results show that the present method, based on the Knight shift, enables us to separately estimate  $p$  for each CuO<sub>2</sub> plane in multilayered high- $T_c$  cuprates.

## EXPERIMENTAL DETAILS

Polycrystalline powder samples of Ba<sub>2</sub>CaCu<sub>2</sub>O<sub>4</sub>(F,O)<sub>2</sub> (0212F) and Ba<sub>2</sub>Ca<sub>2</sub>Cu<sub>3</sub>O<sub>6</sub>(F,O)<sub>2</sub> (0223F), which are listed in Table I, were prepared by high-pressure synthesis, as described elsewhere [29–31]. The crystal structures are shown in Fig. 1(a) and in Fig. 3(a). Powder X-ray diffraction analysis shows that these compounds com-

TABLE I. List of samples measured in this study, bi-layered  $\text{Ba}_2\text{CaCu}_2\text{O}_4(\text{F},\text{O})_2$  (0212F) and three-layered  $\text{Ba}_2\text{Ca}_2\text{Cu}_3\text{O}_6(\text{F},\text{O})_2$  (0223F).  $T_c$  was determined by the onset of SC diamagnetism using a dc SQUID magnetometer. The values of  $p$  for 0212F are evaluated using  $T_c = T_{c,max}[1 - 82.6(p - 0.16)^2]$  [11]. For three-layered 0223F, two values of  $K_{s,ab}$ (300 K) and of  $B$  correspond to OP/IP.

Sample	$T_c$ (K)	$p$	$K_{s,ab}$ (300 K) (%)	$B$ (kOe)
0212F(#1)	102	0.174	0.38	80
0212F(#2)	105	0.149	0.33	74
0212F(#3)	73	0.114	0.25	67
0212F(#4)	40	0.085	0.20	67
0223F	120		0.349/0.275	72/67

prise almost a single phase, and that the  $a$ -axis length continually decreases with an increase in the nominal fraction of  $\text{O}^{2-}$  [31].  $T_c$  was uniquely determined by the onset of SC diamagnetism using a dc SQUID magnetometer. Four 0212F samples exhibit a systematic change in  $T_c$ , as the nominal fraction of oxygen  $\text{O}^{2-}$  decreases at the apical fluorine  $\text{F}^{1-}$  sites, i.e., the hole doping level decreases. Note that the actual fraction of  $\text{F}^{1-}$  and  $\text{O}^{2-}$  is difficult to determine [31–33]. In Table I, the hole density  $p$  is evaluated by using  $T_c = T_{c,max}[1 - 82.6(p - 0.16)^2]$  [11]. For NMR measurements, the powder samples were aligned along the  $c$ -axis in an external field  $H$  of  $\sim 16$  T and fixed using stycast 1266 epoxy. The NMR experiments were performed by a conventional spin-echo method in the temperature ( $T$ ) range of 4.2 – 300 K with  $H$  perpendicular or parallel to the  $c$ -axis. The width of the first exciting  $\pi/2$ -pulse was 6  $\mu\text{s}$ . The  $H$  was calibrated by using the  $^{27}\text{Al}$  Free Induction Decay signal.

## RESULTS

### Bi-layered $\text{Ba}_2\text{CaCu}_2\text{O}_4(\text{F},\text{O})_2$

#### $^{63}\text{Cu}$ -NMR with $H \parallel ab$

Figure 1(b) shows a typical  $^{63}\text{Cu}$ -NMR spectrum of the central transition ( $1/2 \leftrightarrow -1/2$ ) for 0212F(#1), which has the largest nominal  $\text{O}^{2-}$  composition among the bi-layered samples used in this study. The field-swept NMR spectrum was measured at  $H$  perpendicular to the  $c$ -axis ( $H \parallel ab$ ). Here, the NMR frequency  $\omega_0$  was fixed at 174.2 MHz. According to the second order perturbation theory for the nuclear Hamiltonian [34, 35], total NMR shifts consist of the Knight shift  $K_{ab}$  with  $H \parallel ab$  and the second order quadrupole shift as

$$\frac{\omega_0 - \gamma_N H_{res}}{\gamma_N H_{res}} = K_{ab} + \frac{3\nu_Q^2}{16(1 + K_{ab})} \frac{1}{(\gamma_N H_{res})^2}, \quad (1)$$

where  $\gamma_N$  is a nuclear gyromagnetic ratio,  $H_{res}$  an NMR resonance field, and  $\nu_Q$  the nuclear quadrupole frequency.

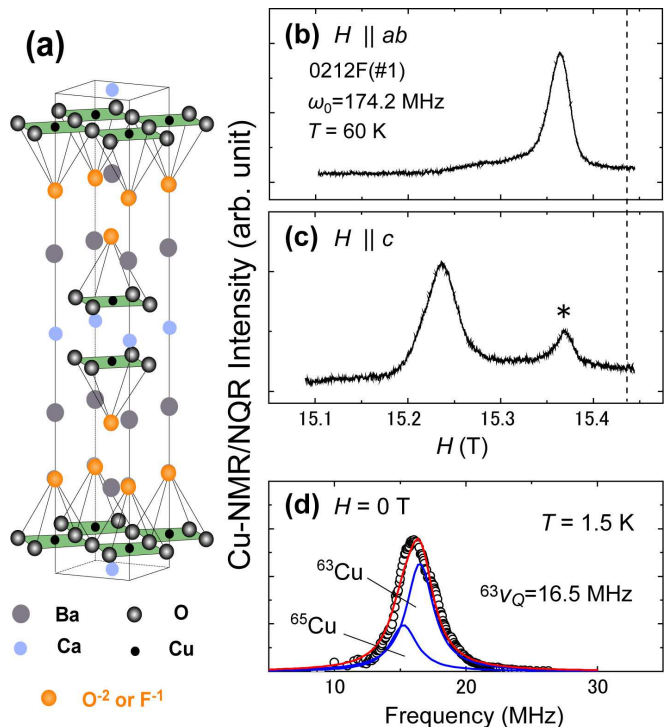


FIG. 1. (color online) (a) Crystal structure of bi-layered  $\text{Ba}_2\text{CaCu}_2\text{O}_4(\text{F},\text{O})_2$  (0212F). The heterovalent substitution of  $\text{O}^{2-}$  for  $\text{F}^{1-}$  increases the hole density. (b)  $^{63}\text{Cu}$ -NMR spectra for 0212F(#1) at  $T=60$  K with  $H$  perpendicular to the  $c$ -axis ( $H \parallel ab$ ). The dashed line points to  $K=0$ . (c)  $^{63}\text{Cu}$ -NMR spectra for 0212F(#1) at  $T=60$  K with  $H$  parallel to the  $c$ -axis ( $H \parallel c$ ). The peak marked with an asterisk (\*) is from unoriented grains with  $\theta \sim 90^\circ$ , where  $\theta$  is the angle between  $H$  and the  $c$ -axis. If  $\theta$  in the unoriented grains were under the completely random distribution, the peak (\*) could coincide with the spectral peak in (b). (d) Cu-NQR spectrum at  $T=1.5$  K. The spectrum is composed of  $^{63}\text{Cu}$  and  $^{65}\text{Cu}$ .

In order to subtract  $K_{ab}$  from the total NMR shift, we estimated the  $\nu_Q$  by nuclear quadrupole resonance (NQR) measurements at  $H=0$  T and  $T=1.5$  K. The NQR spectrum for 0212F(#1) is shown in Fig. 1(d), which has the  $^{63}\text{Cu}$  and  $^{65}\text{Cu}$  components. The  $^{63}\nu_Q$  of  $^{63}\text{Cu}$  is esti-

mated to be 16.5 MHz by the spectral fitting shown in the figure. For other bi-layered compounds, the values of  ${}^{63}\nu_Q$  are 15.7, 13.7, and 12.5 MHz for 0212F(#2), (#3), and (#4), respectively.

Figure 2(a) shows the spin part of the Knight shift,  $K_{s,ab}(T)$ , as a function of temperature. The Knight shift  $K$  in high- $T_c$  cuprates comprises a  $T$ -dependent spin part  $K_s(T)$  and a  $T$ -independent orbital part  $K_{orb}$  as follows:

$$K_\alpha = K_{s,\alpha}(T) + K_{orb,\alpha} \quad (\alpha = c, ab), \quad (2)$$

where  $\alpha$  is the direction of  $H$ . We estimate  $K_{orb,ab} \simeq 0.23$  %, assuming  $K_{s,ab} \simeq 0$  at  $T=0$  limit. The value of  $K_{orb,ab}$  is consistent with those in other hole-doped high- $T_c$  cuprates [17, 18, 20, 36]. Upon cooling down to  $T_c$ ,  $K_{s,ab}(T)$  is roughly constant for 0212F(#1), while  $K_{s,ab}(T)$  decreases for the other four samples in association with the opening of pseudogaps [37, 38]. It is well known that the pseudogaps in  $K_{s,ab}(T)$  emerge in underdoped regions, not in overdoped regions [17, 36]. A steep decrease below  $T_c$  for all samples indicates the reduction in spin susceptibility  $\chi_s(T)$  proportional to  $K_{s,ab}(T)$  due to the formation of spin-singlet Cooper pairing. We note here that in hole-doped cuprates  $K_{s,ab}(T)$  at room temperature,  $K_{s,ab}(300\text{ K})$ , increases with hole density  $p$  [13, 17–22]. The values of  $K_{s,ab}(300\text{ K})$  in the 0212F samples are listed in Table. I. The relationship between  $p$  and  $K_{s,ab}(300\text{ K})$  is discussed later.

### ${}^{63}\text{Cu-NMR}$ with $H \parallel c$

Figure 1(c) shows a typical Cu-NMR spectrum of the central transition ( $1/2 \Leftrightarrow -1/2$ ) for 0212F(#1), where the field-swept NMR spectra were measured at  $H$  parallel to the  $c$ -axis ( $H \parallel c$ ) and at  $\omega_0=174.2$  MHz. The small peak denoted by the asterisk (\*) in the higher-field region arises from unoriented grains with  $\theta \sim 90^\circ$ , where  $\theta$  is the angle between  $H$  and the  $c$ -axis.

Figure 2(b) shows the  $T$ -dependence of  $K_{s,c}(T)$ . We estimate  $K_{orb,c} \simeq 1.22$  %, assuming  $K_{s,c} \simeq 0$  at  $T=0$  limit. Note that when  $H \parallel c$ -axis, the second order quadrupole shift, corresponding to the second term in Eq. (1), is zero [34, 35]. The  $K_{s,c}(T)$  in Fig. 2(b) shows a similar  $T$ -dependence with  $K_{s,ab}(T)$  in Fig. 2(a), as reported for other compounds such as Tl- [20, 39], Bi- [21], and Hg-based compounds [27, 40]. It is, however, different from L214 [19],  $\text{YBa}_2\text{Cu}_3\text{O}_{6+x}$  (Y123) [18, 41, 42] and  $\text{YBa}_2\text{Cu}_4\text{O}_8$  (Y124) [43];  $K_{s,c}(T)$  increases below  $T_c$  upon cooling. This inconsistency comes from the difference of hyperfine magnetic fields discussed below.

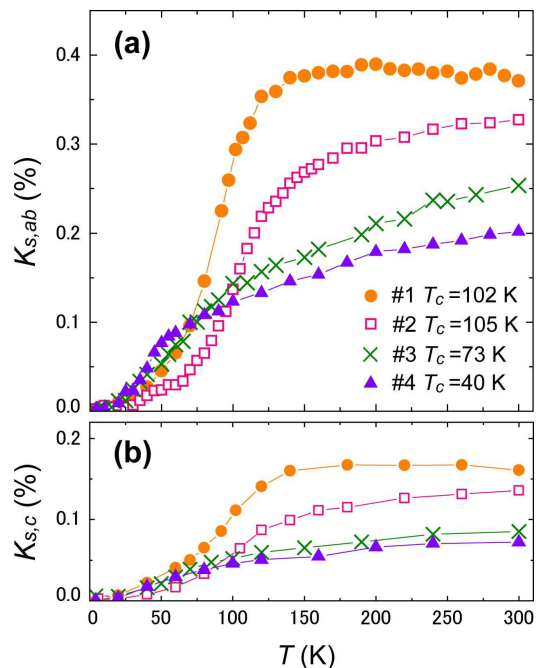


FIG. 2. (color online) (a) Spin part of the  ${}^{63}\text{Cu}$  Knight shift  $K_{s,ab}(T)$  with  $H \parallel ab$  as a function of temperature. The data plots are assigned as labeled in the figure. (b) Spin part of the  ${}^{63}\text{Cu}$  Knight shift  $K_{s,c}(T)$  with  $H \parallel c$ .  $K_{s,c}(T)$  shows the similar  $T$ -dependence with  $K_{s,ab}(T)$ .

### Hyperfine magnetic field in $\text{CuO}_2$ plane

According to the Mila-Rice Hamiltonian [26], the spin Knight shift of Cu in the  $\text{CuO}_2$  plane is expressed as

$$K_{s,\alpha}(T) = (A_\alpha + 4B)\chi_s(T) \quad (\alpha = c, ab), \quad (3)$$

where  $A_\alpha$  and  $B$  are the on-site and the supertransferred hyperfine fields of Cu, respectively. Here, the  $A_\alpha$  consists of the contributions induced by on-site Cu  $3d_{x^2-y^2}$  spins – anisotropic dipole, spin-orbit, and isotropic core polarization; and the  $B$  originates from the isotropic  $4s$  spin polarization produced by neighboring four Cu spins through the  $\text{Cu}(3d_{x^2-y^2})\text{-O}(2p\sigma)\text{-Cu}(4s)$  hybridization. Since the spin susceptibility  $\chi_s(T)$  is assumed to be isotropic, the anisotropy  $\Delta$  of  $K_{s,\alpha}(T)$  is given by

$$\Delta \equiv \frac{K_{s,c}(T)}{K_{s,ab}(T)} = \frac{A_c + 4B}{A_{ab} + 4B}. \quad (4)$$

From Fig. 2,  $\Delta$  is evaluated as  $\sim 0.42$ ,  $0.38$ ,  $0.33$ , and  $0.33$  for 0212F(#1), 0212F(#2), 0212F(#3), and 0212F(#4), respectively. The on-site hyperfine fields,  $A_{ab} \sim 37\text{ kOe}/\mu_B$  and  $A_c \sim -170\text{ kOe}/\mu_B$  [44–46], are assumed as material-independent in hole-doped high- $T_c$  cuprates, which allows us to estimate  $B$  for 0212F samples as listed in Table I. These  $B$  values are larger than  $B \sim 40\text{ kOe}/\mu_B$ , which is a typical value for L214 [19], Y123 [18, 41, 42], and Y124 [43] compounds.

### Three-layered $\text{Ba}_2\text{Ca}_2\text{Cu}_3\text{O}_6(\text{F},\text{O})_2$

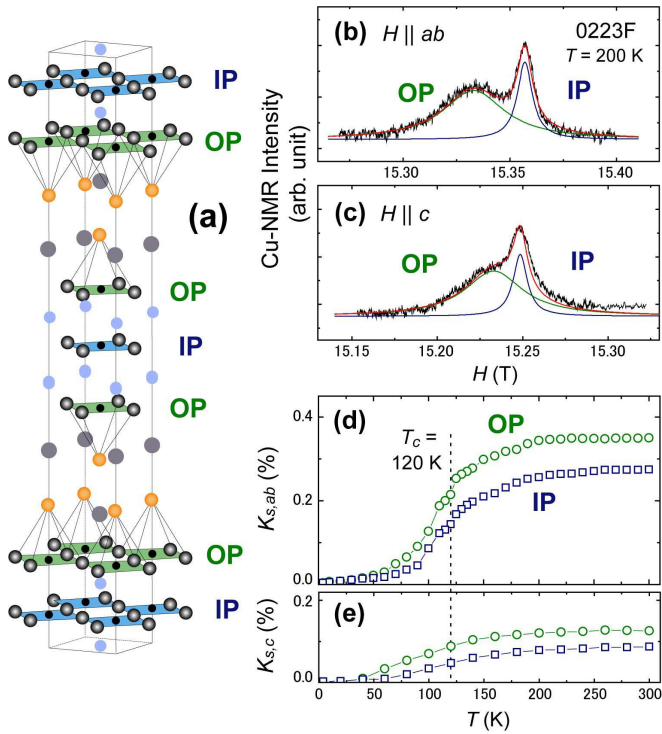


FIG. 3. (color online) (a) Crystal structure of three-layered  $\text{Ba}_2\text{Ca}_2\text{Cu}_3\text{O}_6(\text{F},\text{O})_2$  (0223F). In a unit cell, there are two kinds of  $\text{CuO}_2$  planes: outer  $\text{CuO}_2$  plane (OP) and inner  $\text{CuO}_2$  plane (IP). (b,c) Cu-NMR spectrum of 0223F at  $T=200$  K with  $H \parallel ab$  and  $H \parallel c$ . The spectra have two components arising from OP and IP. (d,e)  $T$ -dependences of  $K_{s,ab}(T)$  and  $K_{s,c}(T)$  for 0223F.

Figures 3(b) and 3(c) show the Cu-NMR spectra of the central transition ( $1/2 \leftrightarrow -1/2$ ) for three-layered  $\text{Ba}_2\text{Ca}_2\text{Cu}_3\text{O}_6(\text{F},\text{O})_2$  (0223F) at  $T=200$  K. The field-swept NMR spectra in Figs. 3(a) and 3(b) were measured at  $H \parallel ab$  and  $H \parallel c$ , respectively. Here, the NMR frequency  $\omega_0$  was fixed at 174.2 MHz. As shown in the crystal structure of 0223F in Fig. 3(a), multilayered compounds, which have more than three  $\text{CuO}_2$  planes in a unit cell, are composed of two kinds of  $\text{CuO}_2$  planes: outer  $\text{CuO}_2$  plane (OP) and inner  $\text{CuO}_2$  plane (IP). The NMR spectra in Figs. 3(b) and 3(c) were assigned to OP and IP as denoted in the figure according to the literature [47]. The NMR spectral width for OP is much broader than that for IP; OP is closer to the Ba-F layer (see Fig. 3(a)), which is the source of the disorder due to the atomic substitution at apical-F sites.

Figures 3(d) and 3(e) show the  $T$ -dependences of  $K_{s,ab}(T)$  and  $K_{s,c}(T)$  for 0223F, respectively. Above  $T_c=120$  K, both  $K_{s,ab}$  and  $K_{s,c}$  decrease upon cooling  $T$  due to the opening of pseudogaps, which suggests that both OP and IP are underdoped. As mentioned before in connection with Fig. 2(a),  $K_{s,ab}(300\text{ K})$  increases with  $p$ .

Therefore, Fig. 3(d) suggests that  $p(\text{OP})$  is larger than  $p(\text{IP})$  in 0223F. The estimation of hole density in multilayered cuprates is discussed later. The anisotropy  $\Delta$  is evaluated from  $K_{s,ab}(T)$  and  $K_{s,c}(T)$  (see Eq. (4)), as conducted in bi-layered 0212F samples.  $\Delta(\text{OP})$  and  $\Delta(\text{IP})$  are evaluated as  $\sim 0.36$  and  $\sim 0.32$ , which provide  $B(\text{OP}) \sim 72 \text{ kOe}/\mu_B$  and  $B(\text{IP}) \sim 67 \text{ kOe}/\mu_B$ .

## DISCUSSIONS

### $p$ dependence of $K_{s,ab}(300\text{ K})$ , $B$ , and $\chi_s(300\text{ K})$ in plane Cu site

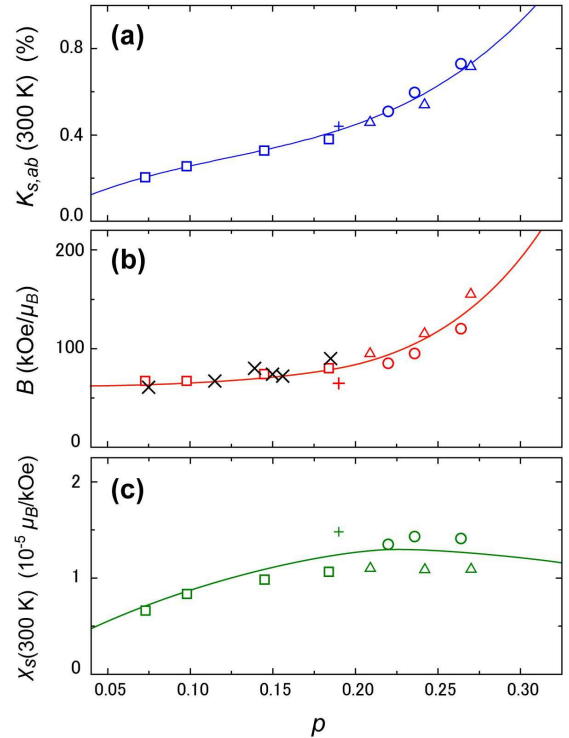


FIG. 4. (color online) (a)  $K_{s,ab}(300\text{ K})$  and (b)  $B$  are plotted as a function of  $p$  for 0212F ( $\square$ ), Bi2212 ( $+$ ), Tl2201 ( $\triangle$ ), and Tl1212 ( $\circ$ ). The values of  $p$  are estimated from  $T_c=T_{c,max}[1 - 82.6(p - 0.16)^2]$  [11]. The plots denoted by crosses ( $\times$ ) in (b) are for multilayered compounds, which are listed in Table II. (c)  $p$ -dependence of  $\chi_s(300\text{ K})$  evaluated from  $K_{s,ab}=(A_{ab} + 4B)\chi_s$  (Eq. (3)). The solid lines in the figures are guides to the eye.

Figure 4(a) shows  $K_{s,ab}(300\text{ K})$  for 0212F,  $\text{Bi}_2\text{Sr}_2\text{CaCu}_2\text{O}_8$  (Bi2212) [36],  $\text{Tl}_2\text{Ba}_2\text{CuO}_{6+\delta}$  (Tl2201) [48], and  $\text{TlSr}_2\text{CaCu}_2\text{O}_{7-\delta}$  (Tl1212) [20] plotted against the  $p$  evaluated by using  $T_c=T_{c,max}[1 - 82.6(p - 0.16)^2]$  [11]. We note that those compounds have one or two  $\text{CuO}_2$  planes with tetragonal symmetry, which are homologous series of the apical-F, Tl-, and Hg-based multilayered compounds. As shown in Fig. 4(a),  $K_{s,ab}(300\text{ K})$  monotonically increases with  $p$  from underdoped to overdoped regions.  $K_{s,ab}(300\text{ K})$  seems



material-independent, suggesting that  $K_s(300\text{ K})$  is a good indication of  $p$  in hole-doped cuprates. If the validity of the  $K_{s,ab}(300\text{ K})$ - $p$  relationship is presented, we can apply it to the estimation of  $p$  in multilayered compounds.

According to Eq. (3), the  $p$  dependence of  $K_{s,ab}(300\text{ K})$  is derived from those of  $B$  and  $\chi_s(300\text{ K})$ . Figure 4(b) shows the  $p$  dependence of  $B$  for the same materials shown in Fig. 4(a) [20, 36, 48]. As presented in Fig. 4(b),  $B$  increases with  $p$ , showing a steep increase at  $p \sim 0.18$ - $0.20$ . It is remarkable that the  $B$  term exhibits weak  $p$ -dependence in the underdoped region, while it shows a steep increase with  $p > 0.16$  in the overdoped region. The  $B$  term arises from the  $\text{Cu}(3d_{x^2-y^2})$ - $\text{O}(2p\sigma)$ - $\text{Cu}(4s)$  covalent bonds with the four nearest neighbor Cu sites; therefore, it is expected that the hybridization between  $\text{Cu}(3d_{x^2-y^2})$  and  $\text{O}(2p\sigma)$  orbitals becomes larger as  $p$  increases in an overdoped regime, and that as a result,  $T_c$  starts to decrease. In Fig. 4(b), the  $p$ -dependent  $B$  term seems *material-independent*; however, the  $B$  terms for L214, Y123, and Y124,  $\sim 40\text{ kOe}/\mu_B$ , are relatively small compared with the values shown in Fig. 4(b). This inconsistency is seen in the variation of  ${}^{63}\nu_Q$  in Fig. 5 as well. The  ${}^{63}\nu_Q$  increases with  $p$  for all materials, while, for a given  $p$ , the absolute values for L214 and Y123 are about 2 to 3 times larger than those for others. The values of  ${}^{63}\nu_Q$  depend on the hole number  $n_d$  in  $\text{Cu}(3d_{x^2-y^2})$  orbit and  $n_p$  in  $\text{O}(2p\sigma)$  orbit. Therefore, it is expected that  $n_d$  and  $n_p$  in L214 and Y123 are distributed in a different manner from those in the cuprates presented here, even though  $p$  ( $p=n_d+2n_p-1$ ) is the same between the former and the latter. Actually, it has been reported that  $n_d$  is large in L214 and Y123, which is the reason for the large  $\nu_Q$  [24, 25]. In this context, it is considered that the hybridization between  $\text{Cu}(3d_{x^2-y^2})$  and  $\text{O}(2p\sigma)$  orbitals in L214, Y123, and Y124 is smaller than those in the cuprates presented here, resulting in the  $B$  for the former being remarkably smaller than for the latter. This is probably related to the crystal structures; L214, Y123, and Y124 have orthorhombic crystal structures in superconducting region, while 0212F, Bi2212, Tl2201, and Tl1212 have tetragonal ones. We conclude that the  $p$ -dependence of  $B$  in Fig. 4(b) holds in  $\text{CuO}_2$  planes with tetragonal symmetry.

Figure 4(c) shows the  $p$  dependence of  $\chi_s(300\text{ K})$ , evaluated using  $K_{s,ab}(300\text{ K})=|A_{ab} + 4B|\chi_s(300\text{ K})$  (see Eq. (3)). The  $\chi_s(300\text{ K})$  increases with  $p$  and is nearly constant above  $p \sim 0.20$ - $0.25$ , which is consistent with previous reports [52]. In general, the spin susceptibility  $\chi_s$  is related to the density of states at the Fermi level. Therefore, the reduction of  $\chi_s(300\text{ K})$  in an underdoped regime would be attributed to the emergence of pseudogaps as discussed in previous literature [52].

When we take into account the  $p$ -dependencies of  $B$  and  $\chi_s(300\text{ K})$ , the  $p$ -dependence of  $K_{s,ab}(300\text{ K})$  – a monotonically increasing function – is explained.

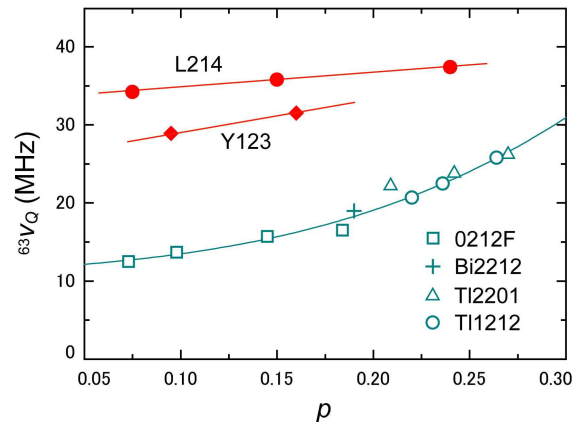


FIG. 5. (color online)  ${}^{63}\text{Cu}$ -NQR frequency  ${}^{63}\nu_Q$  for hole-doped cuprates, 0212F, Bi2212 [36], Tl2201 [49], Tl1212 [20], L214 [19], and Y123 [50, 51]. Here,  $p$  is evaluated from Sr-content  $x$  for L214 and from  $T_{c,max}$  [11] for Y123. The solid lines in the figure are guides to the eye.

In over-doped regimes, a strong hybridization between  $\text{Cu}(3d_{x^2-y^2})$  and  $\text{O}(2p\sigma)$  orbitals increases the  $B$ , making  $K_{s,ab}(300\text{ K})$  larger as  $p$  increases. In under-doped regimes, the opening of the pseudogap decreases  $\chi_s(300\text{ K})$ , making  $K_{s,ab}(300\text{ K})$  smaller as  $p$  decreases. As a result, we conclude that the  $p$ -dependence of  $K_{s,ab}(300\text{ K})$  holds in  $\text{CuO}_2$  planes with tetragonal symmetry. This relationship between  $K_{s,ab}(300\text{ K})$  and  $p$  gives us an opportunity to determine  $p$  separately for OP and IP in multilayered cuprates, if it is confirmed that the relationship holds in multilayered cuprates.

### Hole density estimation in multilayered compounds

In multilayered cuprates, doped hole carriers reside on OP and IP with different doping levels, and the  $\text{CuO}_2$  layers show different physical properties due to the charge distribution even in the same sample. Therefore, it is required to separately estimate  $p$  for OP and IP in order to study the electronic states of multilayered cuprates. It is invalid to apply the estimation methods used in single- and bi-layered compounds, for example, the relationship  $T_c=T_{c,max}[1-82.6(p-0.16)^2]$  [11], the thermoelectric power [9, 10], and the bond valence sums [5–7]. Those methods are applicable to evaluate total hole density, but not to evaluate each hole density at  $\text{CuO}_2$  planes. On the other hand,  $\text{Cu}$ -NMR measures the respective values of  $K_{s,ab}(300\text{ K})$  for OP and IP. If the  $K_{s,ab}(300\text{ K})$ - $p$  relationship in Fig. 4(a) holds even in multilayered cuprates, it allows us to separately estimate  $p$  for OP and IP from experimental values of  $K_{s,ab}(300\text{ K})$ .

Table II lists  $K_{s,ab}(300\text{ K})$ ,  $p'$ , and  $B$  for multilayered cuprates: three-layered 0223F,  $\text{HgBa}_2\text{Ca}_2\text{Cu}_3\text{O}_{8+\delta}$

TABLE II. List of  $K_{s,ab}(300\text{ K})$ ,  $p'$ , and  $B$  for multilayered compounds: three-layered 0223F, Hg1223 [27], and five-layered Hg1245 [28]. Here,  $p'$  is the hole density that is tentatively evaluated by using experimental values of  $K_{s,ab}(300\text{ K})$  and the solid line in Fig. 4(a).

Sample, $T_c$	layer	$K_{s,ab}(300\text{ K})$ (%)	$p'$	$B(\text{kOe}/\mu_B)$
0223F, 120 K	OP	0.35	0.156	72
	IP	0.28	0.115	67
Hg1223, 133 K	OP	0.41	0.185	90
	IP	0.32	0.139	80
Hg1245, 108 K	OP	0.34	0.151	74
	IP	0.21	0.075	61

(Hg1223) [27], and five-layered  $\text{HgBa}_2\text{Ca}_2\text{Cu}_3\text{O}_{12+\delta}$  (Hg1245) [28]. Here,  $p'$  is the hole density tentatively estimated by using the  $K_{s,ab}(300\text{ K})$ - $p$  relationship in Fig. 4(a). We plot  $B$  of those compounds as crosses ( $\times$ ) in Fig. 4(b). The data plots fit into the other data, suggesting that the  $K_{s,ab}(300\text{ K})$ - $p$  relationship is also valid in multilayered cuprates. We may consider the case that the  $K_{s,ab}(300\text{ K})$ - $p$  relationship is modified in multilayered cuprates. According to Eq. (3), the possible source of the modification is the  $p$  dependence of  $B$  or of  $\chi_s$  or both. Experimental  $B$  values in multi-layered compounds, however, fall on the same universal curve as shown in Fig. 4(b); some unexpected modifications on the side of  $\chi_s$  can indeed be considered as unlikely. Therefore, we conclude that the  $K_{s,ab}(300\text{ K})$ - $p$  relationship in Fig. 4(a) is valid for  $\text{CuO}_2$  planes in multilayered compounds, regardless of OP and IP.

Moreover, when we apply the  $K_{s,ab}(300\text{ K})$ - $p$  relationship to five-layered compounds, the fact that the maximum  $T_c$  takes place at  $p \sim 0.16$  [14] supports the validity of the application to multilayered compounds. Several attempts have been used to determine  $p$  of hole-doped cuprates so far – the relationship between  $p$  and  $K_{s,ab}(300\text{ K})$  in this work is a promising approach to estimate  $p$ , which is *applicable to multilayered compounds*. To our knowledge, it is the only method to separately determine  $p$  for OP and IP in multilayered compounds with a reliable accuracy.

## CONCLUSION

We have shown that the planar  $\text{CuO}_2$  hole densities  $p$  in high- $T_c$  cuprates are consistently determined with the Cu-NMR Knight shift. It has been demonstrated that the spin part of the Knight shift  $K_{s,ab}(300\text{ K})$  at room temperature is material-independent in  $\text{CuO}_2$  planes with tetragonal symmetry, and that  $K_{s,ab}(300\text{ K})$  monotonically increases with  $p$  from underdoped to overdoped regions. These observations suggests that  $K_{s,ab}(300\text{ K})$  is a reliable method for determining planar  $\text{CuO}_2$

hole densities. The experimental values of  $K_{s,ab}(300\text{ K})$  and of hyperfine magnetic fields for three-layered  $\text{Ba}_2\text{Ca}_2\text{Cu}_3\text{O}_6(\text{F},\text{O})_2$  and other multilayered compounds support the application of the  $p$ - $K_s(300\text{ K})$  relationship to multilayered compounds. We remark that, to our knowledge, the relationship is the only method to separately determine  $p$  for OP and IP in multilayered compounds with a reliable accuracy.

## ACKNOWLEDGEMENT

The authors are grateful to M. Mori for his helpful discussions. This work was supported by Grant-in-Aid for Specially promoted Research (20001004) and by the Global COE Program (Core Research and Engineering of Advanced Materials-Interdisciplinary Education Center for Materials Science) from the Ministry of Education, Culture, Sports, Science and Technology (MEXT), Japan.

---

\* e-mail: shimizu@nmr.mp.es.osaka-u.ac.jp

- [1] M. W. Shafer, T. Penney, and B. L. Olson, Phys. Rev. B **36**, 4047 (1987).
- [2] K. Kishino, J.-i. Shimoyama, T. Hasegawa, K. Kitazawa, and K. Fueki, Jpn. J. Appl. Phys. **26**, L1228 (1987).
- [3] Y. Tokura, J. B. Torrance, T. C. Huang, and A. I. Nazzal, Phys. Rev. B **38**, 7156 (1988).
- [4] J. B. Torrance, Y. Tokura, A. I. Nazzal, A. Bezinge, T. C. Huang, and S. S. P. Parkin, Phys. Rev. Lett. **61**, 1127 (1988).
- [5] I. D. Brown, J. Solid State Chem. **82**, 122 (1989).
- [6] R. J. Cava, A. W. Hewat, E. A. Hewat, B. Batlogg, M. Marezio, K. M. Rabe, J. J. Krajewski, W. F. Peck Jr., and L. W. Rupp Jr., Physica C **165**, 419 (1990).
- [7] J. L. Tallon, Physica C **168**, 85 (1990).
- [8] A. A. Kordyuk, S. V. Borisenko, M. S. Golden, S. Legner, K. A. Nenkov, M. Knupfer, J. Fink, H. Berger, L. Forró, and R. Follath, Phys. Rev. B **66**, 014502 (2002).
- [9] S. D. Obertelli, J. R. Cooper, and J. L. Tallon, Phys. Rev. B **46**, 14928 (1992).

- [10] J. L. Tallon, C. Bernhard, H. Shaked, R. L. Hitterman, and J. D. Jorgensen, *Phys. Rev. B* **51**, R12911 (1995).
- [11] M. R. Presland, J. L. Tallon, R. G. Buckley, R. S. Liu, and N. E. Flower, *Physica C* **176**, 95 (1991).
- [12] Y. Tokunaga, K. Ishida, Y. Kitaoka, K. Asayama, K. Tokiwa, A. Iyo, and H. Ihara, *Phys. Rev. B* **61**, 9707 (2000).
- [13] H. Kotegawa, Y. Tokunaga, K. Ishida, G.-q. Zheng, Y. Kitaoka, H. Kito, A. Iyo, K. Tokiwa, T. Watanabe, and H. Ihara, *Phys. Rev. B* **64**, 064515 (2001).
- [14] H. Mukuda, Y. Yamaguchi, S. Shimizu, Y. Kitaoka, P. M. Shirage, and A. Iyo, *J. Phys. Soc. Jpn.* **77**, 124706 (2008).
- [15] S. Shimizu, H. Mukuda, Y. Kitaoka, H. Kito, Y. Kodama, P. M. Shirage, and A. Iyo, *J. Phys. Soc. Jpn.* **78**, 064075 (2009).
- [16] S. Shimizu, S.-i. Tabata, H. Mukuda, Y. Kitaoka, P. M. Shirage, H. Kito, and A. Iyo, arXiv:1102.5282, *J. Phys. Soc. Jpn.* (to be published, Vol. 80, No. 4).
- [17] K. Fujiwara, Y. Kitaoka, K. Asayama, Y. Shimakawa, T. Manako, and Y. Kubo, *J. Phys. Soc. Jpn.* **59**, 3459 (1990).
- [18] R. E. Walstedt, W. W. Warren, Jr., R. F. Bell, R. J. Cava, G. P. Espinosa, L. F. Schneemeyer, and J. V. Waszczak, *Phys. Rev. B* **41**, 9574 (1990).
- [19] S. Ohsugi, Y. Kitaoka, K. Ishida, G.-q. Zheng, and K. Asayama, *J. Phys. Soc. Jpn.* **63**, 700 (1994).
- [20] K. Magishi, Y. Kitaoka, G.-q. Zheng, K. Asayama, T. Kondo, Y. Shimakawa, T. Manako, and Y. Kubo, *Phys. Rev. B* **54**, 10131 (1996).
- [21] K. Ishida, K. Yoshida, T. Mito, Y. Tokunaga, Y. Kitaoka, K. Asayama, A. Nakayama, J. Shimoyama, and K. Kishio, *Phys. Rev. B* **58**, R5960 (1998).
- [22] J. G. Storey, J. L. Tallon, and G. V. M. Williams, *Phys. Rev. B* **76**, 174522 (2007).
- [23] Y. Tokunaga, H. Kotegawa, K. Ishida, G.-q. Zheng, Y. Kitaoka, K. Tokiwa, A. Iyo, and H. Ihara, *J. Low Temp. Phys.* **117**, 314 (1999).
- [24] G.-q. Zheng, Y. Kitaoka, K. Ishida, and K. Asayama, *J. Phys. Soc. Jpn.* **64**, 2524 (1995).
- [25] J. Haase, O. P. Sushkov, P. Horsch, and G. V. M. Williams, *Phys. Rev. B* **69**, 094504 (2004).
- [26] F. Mila and T. M. Rice, *Phys. Rev. B* **40**, 11382 (1989).
- [27] K. Magishi, Y. Kitaoka, G.-q. Zheng, K. Asayama, K. Tokiwa, A. Iyo, and H. Ihara, *J. Phys. Soc. Jpn.* **64**, 4561 (1995).
- [28] H. Kotegawa, Y. Tokunaga, Y. Araki, G.-q. Zheng, Y. Kitaoka, K. Tokiwa, K. Ito, T. Watanabe, A. Iyo, Y. Tanaka, and H. Ihara, *Phys. Rev. B* **69**, 014501 (2004).
- [29] A. Iyo, Y. Tanaka, M. Tokumoto, and H. Ihara, *Physica C* **366**, 43 (2001).
- [30] A. Iyo, M. Hirai, K. Tokiwa, T. Watanabe, and Y. Tanaka, *Physica C* **392**, 140 (2003).
- [31] P. M. Shirage, D. D. Shivagan, Y. Tanaka, Y. Kodama, H. Kito, and A. Iyo, *Appl. Phys. Lett.* **92**, 222501 (2008).
- [32] S. Shimizu, H. Mukuda, Y. Kitaoka, A. Iyo, Y. Tanaka, Y. Kodama, K. Tokiwa, and T. Watanabe, *Phys. Rev. Lett.* **98**, 257002 (2007).
- [33] S. Shimizu, T. Sakaguchi, H. Mukuda, Y. Kitaoka, P. M. Shirage, Y. Kodama, and A. Iyo, *Phys. Rev. B* **79**, 064505 (2009).
- [34] A. Abragam, in *The Principles of Nuclear Magnetism* (Clarendon, Oxford, 1961).
- [35] M. Takigawa, P. C. Hammel, R. H. Heffner, Z. Fisk, J. L. Smith, and R. B. Schwarz, *Phys. Rev. B* **39**, 300 (1989).
- [36] K. Ishida, Y. Kitaoka, K. Asayama, K. Kadowaki, and T. Mochiku, *J. Phys. Soc. Jpn.* **63**, 1104 (1994).
- [37] H. Yasuoka, T. Imai, and T. Shimizu, in *Strong Correlation and Superconductivity*, edited by H. Fukuyama, S. Maekawa, and A. P. Malozemoff (Springer, Berlin, 1989) Vol. 89, p. 254.
- [38] R. E. Walstedt, in *The NMR Probe of High- $T_c$  Materials* (Springer, Berlin, 2008).
- [39] Y. Kitaoka, K. Fujiwara, K. Ishida, K. Asayama, Y. Shimakawa, T. Manako, and Y. Kubo, *Physica C* **179**, 107 (1991).
- [40] M.-H. Julien, M. Horvatić, P. Carretta, C. Berthier, Y. Berthier, P. Ségransan, S. M. Loureiro, and J.-J. Capponi, *Physica C* **268**, 197 (1996).
- [41] S. E. Barrett, D. J. Durand, C. H. Pennington, C. P. Slichter, T. A. Friedmann, J. P. Rice, and D. M. Ginsberg, *Phys. Rev. B* **41**, 6283 (1990).
- [42] M. Takigawa, A. P. Reyes, P. C. Hammel, J. D. Thompson, R. H. Heffner, Z. Fisk, and K. C. Ott, *Phys. Rev. B* **43**, 247 (1991).
- [43] H. Zimmermann, M. Mali, M. Bankay, and D. Brinkmann, *Physica C* **185-189**, 1145 (1991).
- [44] A. J. Millis, H. Monien, and D. Pines, *Phys. Rev. B* **42**, 167 (1990).
- [45] T. Imai, *J. Phys. Soc. Jpn.* **59**, 2508 (1990).
- [46] H. Monien, D. Pines, and M. Takigawa, *Phys. Rev. B* **43**, 258 (1991).
- [47] M.-H. Julien, P. Carretta, M. Horvatić, C. Berthier, Y. Berthier, P. Ségransan, A. Carrington, and D. Colson, *Phys. Rev. Lett.* **76**, 4238 (1996).
- [48] Y. Kitaoka, K. Fujiwara, K. Ishida, K. Asayama, Y. Shimakawa, T. Manako, and Y. Kubo, *Physica C* **176**, 107 (1991).
- [49] K. Fujiwara, Y. Kitaoka, K. Ishida, K. Asayama, Y. Shimakawa, T. Manako, and Y. Kubo, *Physica C* **184**, 207 (1991).
- [50] C. H. Pennington, D. J. Durand, C. P. Slichter, J. P. Rice, E. D. Bukowski, and D. M. Ginsberg, *Phys. Rev. B* **39**, 2902 (1989).
- [51] Y. Yoshinari, H. Yasuoka, Y. Ueda, K.-i. Koga, and K. Kosuge, *J. Phys. Soc. Jpn.* **59**, 3698 (1990).
- [52] J. W. Loram, J. Luo, J. R. Cooper, W. Y. Liang, and J. L. Tallon, *J. Phys. Chem. Solids* **62**, 59 (2001).